# **Supporting Information**

### Egeland et al. 10.1073/pnas.1718678115

#### SI Appendix

Summary of the Sima de los Huesos and Dinaledi Chamber Assemblages. The SH hominin assemblage, which is composed of at least 28 individuals (1), dates between 427 and approximately 600 ka (2, 3) and is deposited along a ramp located at the bottom of a 13-m vertical shaft. Another 17 m of vertical climb and around 500 m of spelunking separates the shaft from the current ground surface (4). Although the depositional history of the remains is controversial, it appears that it represents a single stratigraphic event (5). There is some agreement, too, that the assemblage's formation involves hominin agency. Some suggest, for example, that the corpses were transported into the chamber by large felids after their collection and abandonment by hominins elsewhere within or just outside the cave system (6), while others favor intentional, and perhaps symbolic, caching within the chamber itself (4, 7).

A variety of direct and indirect dating techniques point to an age of approximately 300 ka for the DC hominin remains (8). The bone-bearing deposit, which contains the remains of at least 15 individuals (9), lies along the surface of a gently sloping cavity ~30 m below the current ground surface. Entrance to the DC is currently limited to a 12-m vertical shaft that itself can only be reached after a 50- to 120-m (depending on the route chosen) journey through several narrow access points and a climb over, and back down, a large dolomite block (10). Dirks et al. (10, 11; see also ref. 12) consider several hypotheses to explain the accumulation of hominin remains in the DC and, based on a coalescence of geological and taphonomic data, find the deliberate disposal of the hominin corpses to be the most likely scenario. Another interpretive challenge is posed by the discovery of yet more hominin material within another chamber of the Rising Star Cave System (13).

Comparative Primate Skeletal Collections. We surveyed the literature and, in addition to the SH and DC, identified a sample of 36 hominin/nonhominin primate assemblages where information on the abundance, rather than simple presence/absence, of individual skeletal elements (rather than pooled skeletal groups, such as "limb bone" or "appendicular") is available (Dataset S1). For each assemblage, abundances, as estimated by the minimum number of elements (MNE), are available for a total of 23 elements. To mediate preservation biases due to bone density, we limit our sample when possible to adolescent and adult specimens. This cut-off is based on clinical work that shows the rate of bone mineral density accumulation increases during and after puberty in both females and males (14), a finding that helps explain bioarchaeological observations that adolescent skeletal remains tend to preserve as well as those of adults (15, 16). The samples from Fontbrégoua Feature H1, Fontbrégoua Feature H3, and the DC, all of which are used in the final analysis, include subadolescent remains because skeletal element data are not available by age group. All MNEs are converted into minimum animal units and standardized relative to the most frequent element. Formation of these bone collections results from a variety of observed or inferred processes, and we organize the sample as follows.

Prehistoric assemblages.

**Primary hominin interment.** These assemblages include hominin skeletons found within well-defined, artificial sedimentary structures that clearly indicate intentional burial of complete corpses with little or no evidence of subsequent movement or disturbance.

*Possible primary hominin interment.* These assemblages include hominin skeletons recovered from natural depressions or niches, or within possible but ambiguous artificial sedimentary struc-

tures. These assemblages, all of which derive from caves and rock shelters, also display evidence of subsequent movement or disturbance.

Hominin cannibalism/secondary interment. These assemblages preserve evidence for the anthropogenic modification of hominin corpses in the form of cutmarks, percussion marks, and/or impact fractures. These assemblages may (e.g., El Mirador) or may not (e.g., Gran Dolina) occur within artificial sedimentary structures that indicate secondary interment.

Nonanthropogenic hominin accumulation. These assemblages show no stratigraphic or taphonomic evidence for the deliberate interment or caching of hominin corpses.

#### Modern assemblages.

Unscavenged human corpses. These assemblages result from the deposition of human corpses in modern medico-legal contexts in the Pacific Northwest of the United States. These assemblages show no or very little evidence of scavenging (e.g., little or no disarticulation or scattering and/or few or no carnivore tooth marks). The deposition of these corpses was not observed (17).

Scavenged human corpses. These assemblages also result from the deposition of human corpses in modern medico-legal contexts in the Pacific Northwest of the United States. These assemblages, however, do show evidence of scavenging (e.g., disarticulation, scattering, or carnivore tooth marks). The deposition of these corpses was not observed (17).

Leopard refuse. These assemblages represent the bones that remain after the consumption of modern baboon carcasses by leopards. The formation of these assemblages was observed (18) or inferred through contextual evidence (19).

Misgrot Cave. Because this assemblage has not been published in any detail, we provide a fuller description here. Misgrot (20) is a dolomitic cave (Eccles Formation) near Northam (Limpopo Province, South Africa) that reaches the surface via a near vertical ~17-m shaft (Fig. S1). The cave was investigated in February 2004 by J.L.H. and C.G.M. along with Pedro Boshoff, Hedman Zondo, and the late André Keyser. Among the bones encountered within the cave were abundant baboon (Papio ursinus) remains, which were represented as more-or-less complete skeletons (e.g., an entire mummified male baboon) (Fig. S2) near the cave opening and as more isolated parts as the scatter progressed further down the talus slope (Fig. S3). All bones were identified by ontogenetic age, skeletal element, and side but left in situ because one of the goals of the 2004 investigation was to track longitudinal changes in element disarticulation and movement. The only nonbaboon remains identified in the in situ assemblage were a partial mandible of a lion (Panthera leo) and a mummified, nearly complete rock hyrax (Procavia capensis). Since 2004, the cave has been 3D-mapped, camera traps put in place, and additional remains excavated. The camera traps and the immense accumulation of dung indicate that baboons do indeed live in and around the cave, which suggests that the deposition of the carcasses before 2004 resulted largely, if not exclusively, from baboon cave use. While a definitive inventory must await the maceration of the excavated assemblage, we present here preliminary skeletal element frequencies from the baboon bones identified in situ in 2004.

Unfortunately, many of the comparative assemblages are of limited utility for robust statistical analysis. Low minimum number of individual (MNI) counts and high frequencies of missing values (i.e., the complete absence of skeletal elements from an assemblage) in particular produce significant variance heterogeneity both between and among assemblage types as

determined through Brown–Forcythe and Hartley's tests. The retention of only those skeletal element data that result in variance homogeneity (the only exception to this is Gran Dolina Level TD6, which we preserve in the final analysis because of the rarity of inferred Pleistocene cases of cannibalism), then, yields a sample of 14 assemblages for comparison with the SH and DC.

**Primate Skeletal Element Data.** Below is a summary of the skeletal element data from each of the 38 primate assemblages. The 14 assemblages included in the multivariate statistical analyses (Table S1) are marked with an asterisk (\*), and we provide additional details on their taphonomic histories and chronology. **Primary hominin interment.** 

**Pottery Mound: Pueblo IV component\*.** Data are from table 1 in Trinkaus (21) and are limited to elements with age-at-death estimates of 14 y or older. Cranial MNE is based on neurocrania and does not include teeth.

Pottery Mound is a large Pueblo IV adobe village that lies atop a low hill overlooking the Rio Puerco in New Mexico, United States. The primary occupation of the site, which occurred between about AD 1370 and AD 1450 (22), is well-known for its spectacular kiva murals (23). A total of 110 burials with skeletal remains reported to be "relatively well preserved" were excavated from within rooms and kivas and along the sides of the mound (24).

Kuaua Pueblo: Pueblo IV component\*. Data are from table 1 in Trinkaus (21) and are limited to elements with age-at-death estimates of 14 y or older. Cranial MNE is based on neurocrania and does not include teeth.

Kuaua Pueblo is a large adobe village that overlooks the west bank of the Rio Grande in New Mexico. Village construction began in the mid- to late 14th century AD and the site was fully abandoned near the end of the 17th century AD (25). Nearly 300 burials are reported from the site, and among the 100 for which details are available, a vast majority were recovered from room contexts and are described as "a hole...just large enough to hold the flexed body" (26).

Hummingbird Pueblo: Pueblo I component. Data are from table B1-B in Karhu (27) and include skeletons from Features 42.02, 42.03, 42.05, 71.01, 75.01, and 79. Only skeletons with age-at-death estimates of 20 y or older are included. For Feature 79, a total of 39 elements is listed under "hand phalanges" in table B1-B of Karhu (27). Because this represents more phalanges than are found in two complete hands, we assume that the remaining 11 are pedal phalanges.

**Dolni Věstonice I DV 3.** Data are from table 16.5 in Trinkaus (28), table 18.1 in Trinkaus (29), and table 5.6 in Holliday et al. (30). Holliday (31) states that the DV 3 rib cage is still embedded in matrix, and we assume here that all of the ribs are present. The DV 3 individual is classified as a middle-aged adult (32).

**Dolní Věstonice II triple burial.** Data are from table 16.5 in Trinkaus (28), table 18.1 in Trinkaus (29), and tables 5.5 and 5.7 in Holliday et al. (30). Only skeletons DV 13 and DV 15, both of which have age-at-death estimates of 20 y or older (32), are included.

Possible primary hominin interment.

Mugharet es-Skhūl: Layer B\*. Data are from McCown and Keith (33). Only Skhūl II, Skhūl III, Skhūl IV, Skhūl V, Skhūl VI, and Skhūl VII, all of which are listed as "adult" or have age-at-death estimates of 20 y or older, are included. For Skhūl IV, McCown and Keith (33) list as present "fragments of the dorsal [thoracic] vertebrae" but that "the only relatively complete specimens are the eleventh and twelfth." We assume here that all 12 thoracics are present. For Skhūl V, five middle phalanx fragments are identified (33), and we assume that each fragment represents a separate element. The pelvis of Skhūl VI is represented by "[s] everal fragments whose position is uncertain" (33). We assume that both the right and left innominates are represented by these fragments.

The early modern human remains from Layer B of es-Skhūl (Israel) date to MIS 5, approximately 100–135 ka (34). Parts of 10 skeletons (in addition to 16 isolated specimens) were recovered from Layer B. While there is no clear stratigraphic evidence that any of the skeletons were deposited in artificially excavated pits, seven show some degree of natural articulation. In his report on the excavation of the remains, McCown (35) argues that a strong case for intentional burial can only be made for Skhūl I, Skhūl IV, Skhūl V, and Skhūl VII, although later syntheses consider not only these four but seven or even all 10 partial skeletons to be burials (36, 37).

Djebel Qafzeh: Couche XVII. Data are from Vandermeersch (38). Only skeletons listed as "adult" or with an age-at-death estimate of 20 y or older (Q8 and Q9) are included. While the trunk and vertebral column of Q9 is crushed (38), we assume, given that the skeleton is mainly complete, that all of the vertebrae and ribs are present.

**Regourdou.** Data are from tables 1 and 2 in Madelaine et al. (39) and tables S2 and S3 in Gómez-Olivencia et al. (40). Only Regourdou 1, aged as an adult, is included.

*La Chappelle-aux-Saints.* Data are from table 2 in Gómez-Olivencia (41) and figure S9 in Rendu et al. (42). These data include only the adult LCS 1 skeleton.

Mugharet et-Tabūn: Layer C. Data are from McCown and Keith (33). Only the Tabūn I skeleton, which is identified as an adult, is included.

Shkaft Mazin Shanidar: Layer D Upper. Data are from Trinkaus (43) and include the Shanidar 1, 3, and 5 skeletons, all of which are identified as adult. Trinkaus (43) states that Shanidar 1 could be represented by either 10 or 11 thoracic vertebrae. We use the lower value here. Reynolds et al. (44) report the discovery of additional hominin material that, they argue, likely belongs to Shanidar 5. We include these specimens in the element frequencies for Shanidar 5.

Shkaft Mazin Shanidar: Layer D Lower. Data are from Trinkaus (43) and include the Shanidar 2, 4, 6, and 8 skeletons, all of which are identified as adult.

Mugharet el-Kebara: Couche XII. Data are from Tillier (45), Arensburg (46), Rak (47), and Vandermeersch (48). These data include only the adult Kebara 2 skeleton.

El Mirón Cave. Data are from table 1 in Carretero et al. (49). These data include only the El Mirón 1 adult skeleton.

Hominin cannibalism/secondary interment.

*Krapina\**. Data are from table 1 in Trinkaus (21) and are limited to elements with age-at-death estimates of 14 y or older. Cranial MNE is based on neurocrania and does not include teeth. The hominin remains derive from several stratigraphic layers. While the stratigraphic provenience for some of the crania and mandibles is known (table 4 in ref. 50), that of the postcranial remains, as Trinkaus (51) laments, is unknown. We therefore necessarily lump the entire hominin sample into a single analytical unit.

The Neandertal remains from the Hušnjakovo rock shelter just outside the town of Krapina (Croatia) date to MIS 5e, approximately 130 ka (52). Interpretations of the Krapina hominins' depositional history vary. Trinkaus (21) observes that the skeletons, while disassociated and broken, are represented by nearly all elements, including relatively fragile bones, which suggests rapid burial of the bodies, either through natural processes (e.g., rockfall) or intentional interment. The fragmentary nature of the collection could be explained, he hypothesizes, by postdepositional disturbance or, perhaps, partial disarticulation of the corpses by hominins before burial. Ullrich (53) favors the latter possibility and argues further that hominins harvested the bones of the deceased to engage in ritual defleshing, disarticulation, and breakage. These and other interpretations, including the long-established cannibalism model (54, 55), hinge in part on the frequency, and even correct identification, of perimortem cutmarks and breakage, all of which are disputed (21, 53, 56, 57).

Fontbrégoua: Feature H1\*. Data are from table 3 in Villa et al. (58). The feature contains skeletal remains from a minimum of seven individuals: three adults and four children. However, skeletal element frequencies are not reported for each individual, so we use the pooled data here.

The Neolithic cave of Fontbrégoua is located in southwestern France. Feature H1 is a small, artificial sedimentary structure in the southeast corner of the cave that dates to ~4900 B.P. (59). Cutmarks and perimortem fractures are common on the remains, and high frequencies of conjoined pieces suggest that the cluster represents a distinct episode of butchery. Similarities in butchery patterns and skeletal representation between the Feature H1 human bones and the animal bones recovered from other areas of the cave are cited as strong evidence for cannibalism (58), although this interpretation has not gone unchallenged (60, 61).

Fontbrégoua: Feature H3\*. Data are from table 3 in Villa et al. (58). The feature contains skeletal remains from a minimum of six individuals: three adults, two children, and an individual of unknown age-at-death. However, skeletal element frequencies are not reported for each individual, so we use the pooled data here. Villa et al. do not distinguish between radii and ulnae in their MNE estimates. Thus, we arbitrarily divided the total reported MNE of nine into four radii and five ulnae. Villa et al. also do not distinguish among vertebrae in their MNE estimates. We therefore arbitrarily assign the two identified vertebrae as cervicals.

Feature H3 is a small, artificial sedimentary structure located along the north wall of Fontbrégoua cave and also dates to ~4900 B.P. (59). Cutmarks and perimortem fractures are common on the Feature H3 human remains and many of the pieces refit, again suggesting a distinct episode of butchery. Feature H3 is also interpreted as evidence for cannibalism (58).

Gran Dolina: Level TD6\*. Data are from table 1 in Bermúdez de Castro et al. (62, 63), Carretero et al. (64), Gómez-Olivencia et al. (65), Lorenzo et al. (66), and Pablos et al. (67). We include only adult specimens. We assume the following unaged specimens to be adult: a second metatarsal (40, 41), all unaged phalanges (66), a calcaneous (67), and a femur, the latter of which shows no woven bone (64). Mandible MNEs include isolated teeth.

Level TD6 of the Gran Dolina site (Sierra de Atapuerca, Spain) dates between 800 and 900 ka (68). Within the sequence, hominin bones occur randomly scattered among the more numerous animal bones, and both sets of remains preserve numerous butchery marks (69). In fact, the raw frequency of hominin bones with butchery marks is second only to that of cervids (70). Butchery patterns among the hominin and animal remains are broadly similar; the main difference is the presence of peeling damage among the former, an observation that Fernández-Jalvo et al. (69) attribute to the relative ease with which a hominin bone can be broken manually and without recourse to a hammer stone. Taken together, these data form strong support for cannibalism, and because butchered hominin remains occur within distinct subunits of Level TD6, the consumption of hominins was likely not a one-time event (71). What is more, the hominin remains show little or no evidence for carnivore involvement, which contrasts sharply with—and suggests a taphonomic history distinct from—the nonhominin assemblage (72).

El Mirador: MIR4A\*. Data are from table 2 in Cáceres et al. (73) and include only those specimens identified as adult or not explicitly assigned to Individual 1 (a child of about 8 y of age at death).

The cave of El Mirador (Sierra de Atapuerca, Spain) contains a sequence of Bronze Age occupations. Level MIR4A contains human remains with butchery marks, human tooth marks, extensive green breakage, and cooking damage, all of which strongly suggest cannibalism. The bones, which date to the Early Bronze

Age (ca. 4200 B.P.), were later collected by Middle Bronze Age (ca. 3400 B.P.) occupants and placed in a small pit for secondary burial (73).

Gough's Cave: Magdalenian occupation. Data are from table 2 and SOM figures 1, 2, 6–15 in Bello et al. (74), Hawkey (75), and Churchill (76). Those specimens classified as adult or "adult?" are included.

5MT-3: Mancos Component. Data are from table 1 in Malville (77). The feature contains skeletal remains from a minimum of 10 individuals: 6 adults and 4 children. However, skeletal element frequencies are not reported for each individual, so we use the pooled data here. Malville does not distinguish between manual and pedal phalanges, so we divide the pooled phalanx MNE by two to derive abundances for these two elements. Cranial and mandible MNEs do not include isolated teeth.

5MT-10010: Feature 3. Data are from table 6 in Billman (78) and table 2 in Lambert et al. (79). The feature contains skeletal remains from a minimum of five individuals: four adults and one adolescent aged 11 y. However, the frequencies are reported by individual for some, but not all, elements (compare, for example, table 5 in ref. 48 with table 2 in ref. 49), so we use the pooled data here.

La Tolita: Cama de Huesos. Data are from Ubelaker (80). Only remains from individuals with age-at-death estimates of 18 y or older are included.

*Crow Creek: Initial coalescent component.* Data are from tables 3 and 4 in Willey (81). Only remains from individuals with age-atdeath estimates of 18 y or older are included. Cranial MNE is based on Willey's minimum count of temporal bones.

Nonanthropogenic hominin accumulation.

A.L. 333: Denen Dora Member\*. Data are from Kimbel et al. (82), White and Johanson (83), Lovejoy et al. (84–86), Ward et al. (87,

88), Bush et al. (89), and Latimer et al. (90) and include only those specimens identified as adult or not explicitly aged as subadults.

The Denen Dora Member of the Hadar Formation (Ethiopia) dates to ~3.2 Mya (91). While many of the hominin remains are surface finds, those fossils that derive from an excavated context appear in clayey silts (92) that were deposited in a low-energy depositional environment, perhaps as the result of a shallow

depositional environment, perhaps as the result of a shallow seasonal flood (93). It is therefore unlikely that the hominins were overwhelmed and buried by a catastrophic flood. The fossils display only light subaerial weathering and are purportedly free of carnivore damage (92, 94, 95), so the corpses were probably exposed on the landscape for only a short period of time. Except for a partially articulated hand and foot, the skeletons are nonetheless disassociated and incomplete, so some postdepositional disturbance certainly occurred. Pettitt (36) argues, somewhat controversially, that the A.L. 333 assemblage is an example of funerary caching, which he defines in part as "the structured deposition of a corpse, or part of a corpse, in a chosen place, without modification of that place" and, as such, "is given meaning beyond prosaic concerns such as corpse protection." The evaluation of this and other scenarios awaits a full taphonomic analysis of the remains.

Liang Bua: Layer R. Data are from Brown et al. (96), Morwood and Jungers (table 1 in ref. 97), Larsen et al. (table 1 in ref. 98), Jungers et al. (table 1 in ref. 99), and Morwood et al. (table 1 in ref. 100), and include the LB 1 and 8 partial skeletons, both of which are identified as adult. Vertebrae are listed as "present" by Brown et al. (96) and a single cervical, but no thoracics or lumbars, are listed in the compilation of Morwood and Jungers (table 1 in ref. 97). We thus assign thoracic and lumbar MNEs for LB 1 (one thoracic and one lumbar) based on figure 30.3 in Jungers (101). A sacrum and scapulae are listed as "present" by Brown et al. (96) for LB 1 but neither appears in the compilation of Morwood and Jungers (table 1 in ref. 97), in figure 30.3 in

Jungers (101), or in the descriptions of the upper limb in Larson et al. (98). We therefore assign an MNE of zero for these elements.

Liang Bua: Layer O-Q. Data are from table 1 in Morwood et al. (100), table 1 in Larson et al. (98), table 1 in Jungers et al. (99), and Orr et al. (102). These data include remains from individuals LB 5 and 6, both of which are identified as adult, and LB 13, 20, 21, and 22, all of which are unaged but assumed here to be adult.

*Dmanisi: Layer B1y.* Data are from Lordkipanidze et al. (103–105) and Gabunia et al. (106). Skulls 1 and 2 were recovered from Block 1 without fine stratigraphic control. Here we assume that they derive from Level B1y along with the other adult remains.

Malapa: Facies D. Data are from Berger et al. (table S1 in ref. 107), de Ruiter et al. (108), Churchill et al. (109), Kivell et al. (table S1 in ref. 110), and Zipfel et al. (111) and include only specimens listed as adult. While the two adult left fibulae fragments do not overlap, Berger et al. (table S1 in ref. 107) believe they derive from separate individuals, so we assigned an MNE of two for the fibula.

Unscavenged human corpses: Forensic cases from Washington State, United States\*. Data are from table 7.1 and Appendix A.2 in Haglund (17) and include only those corpses aged 17 y or older at the time of death. The deposition of the corpses was not observed, but, according to Haglund (17), "scattering and loss of unscavenged remains on land was minimal. Skeletons were usually discovered in relative anatomical order. The elements that were removed were most likely the result of opportunistic transport by animals." Haglund (17) also notes that "[u]nscavenged remains provided a baseline of expected survival frequencies without the severe biasing influence imposed by scavenger destruction or loss in water. Skeletal elements that were not recovered from unscavenged remains are most likely the result of collection bias, human interference, or animal transport."

#### Scavenged human corpses.

Forensic cases from Washington State, United States\*. Data are from table 7.1 and Appendix A.2 in Haglund (17) and include only those corpses aged 17 y or older at the time of death. The deposition of the corpses was not observed, but Haglund (17) reports that the "[t]ype of scavenger was inferred by the presence of tooth marks, scattering of bones, scat deposits, and animal tracks at the site where the body was recovered. In some cases, animals were observed feeding on the body or the body was discovered confined with the animal."

Bear-scavenged corpses from New Mexico, United States. Data are from table 1 in Carson et al. (112). The age-at-death for the decedents is not reported; we assume they all represent adults. The deposition of the corpses was not observed. The inference of bear scavenging is based on reports of bears near the skeletal remains and/or the presence of: (i) tooth marks consistent with the size of bear teeth; (ii) bear scat containing human hair, clothing, and bone fragments; and (iii) bear nests near the corpses.

Scavenged corpse from North Carolina, United States. Data collected from a forensic case curated in the biological anthropology laboratory at the University of North Carolina at Greensboro. The remains derive from a middle-aged male recovered from a homeless camp. The bones preserve numerous tooth marks and extensive furrowing from an unknown carnivore. Leopard refuse.

Mapungubwe National Park leopard kills\*. Data are from table 4 in Pickering et al. (19). The assemblage contains skeletal remains from a minimum of seven baboon individuals: a juvenile male, an immature adult male, a young adult female, an adult female, an old adult female, and a very old male. However, skeletal element frequencies are not available for each individual, so we use the pooled data here. Manual and pedal phalanges are not distinguished, so we divide the total phalanx MNE by two to arrive at separate MNE values for manual and pedal phalanges. Neither the kills nor the corpses' deposition was observed. The

inference of leopard involvement is based on park ranger reports, leopard spoor, and a lack of nonleopard taphonomic signatures. However, damage and transport of some bones by small carnivores cannot be ruled out.

Leopard-consumed baboons\*. Data are from table 1 in Pickering and Carlson (18). The assemblage contains skeletal remains from eight baboon individuals: two subadult females, two adult females, one subadult male, one adult male, and two old adult males. However, skeletal element frequencies are not available for each individual, so we use the pooled data here. Manual and pedal phalanges and metacarpals and metatarsals are not distinguished, so we divide the total phalanx/metapodial MNEs by two to arrive at separate MNE values for manual and pedal phalanges and metacarpals and metatarsals. These data include only the "refuse" assemblage from the observed feedings (113). Natural baboon accumulation: Misgrot Cave baboons\*. The assemblage contains skeletal remains from a minimum of seven adult and juvenile baboon individuals. However, skeletal element frequencies are not available for each individual, so we use the pooled data here. Manual and pedal phalanges are not distinguished, so we divide the total phalanx MNE by two to arrive at separate MNE values for manual and pedal phalanges. See discussion above for details on the site's taphonomic history. Possible hominin deliberate disposal.

Sima de los Huesos: Sierra de Atapuerca. Data are from Bermúdez de Castro et al. (table 1 in ref. 1), Arsuaga et al. (table S1 in ref. 114), and Pablos et al. (115–117) and include only those specimens identified as adult or not explicitly listed as subadult.

Dinaledi Chamber: Rising Star Cave System. Data are from Dirks et al. (table 1 in ref. 10) and Feuerriegel et al. (118). In addition to a minimum of four first or second ribs, Dirks et al. (10) list at total of 48 unidentified rib fragments. To arrive at an MNE for ribs, we divided 48 by 2 and then added the result (=24) to the four first or second ribs. Cranial MNE does not include teeth. The DC collection includes remains from individuals ranging in age from infant to adult. However, skeletal element frequencies are not available for each individual, so we used the pooled data here. We note that among the 13 DC individuals associated with age-at-death estimates, seven are classified as "old juvenile" or younger (9), so the attrition of ontogenetically younger, and thus lower-density, skeletal elements may partially mask what originally was more complete skeletal representation.

Statistical Treatment of Primate Skeletal Part Data. All analyses described below are run within the R statistical environment (119). **Exploratory analysis.** The goal of exploratory analysis is twofold: (i) to identify the optimum number of groups represented by the hominin assemblages and (ii) to determine the membership of each identified group. Many grouping algorithms tend to perform poorly when, as is the case here, the number of variables (skeletal elements = 23) substantially exceeds sample size (hominin assemblages = 16). To address this discrepancy, we used a RF analysis on all 16 assemblages, including the SH and DC, to identify a subset of skeletal elements that is smaller than the sample size and explains the greatest amount of variance (120). To identify the optimum number of groups represented by all 16 assemblages, those skeletal elements with a MDA value > 5 after the generation of 500 trees are entered in the "NbClust" R library, which runs and combines 30 different clustering algorithms. A k-means analysis then classifies each of the comparative assemblages into one of the groups recognized by the NbClust functions. The strength of group assignment is assessed with the "clusplot" graphic function, which provides 95% confidence ellipses and silhouette plots, which estimate the s(i) value of each comparative assemblage. A comparison of within- and between-group distances results in s(i) values that range from 1 (strong classification within a group) to 0 (parsimonious but weak classification within a group). This preliminary classification

establishes a framework for the application of a variety of machine-learning methods that can identify the comparative assemblages that best match the hominin concentrations from the SH and DC.

Classifying the SH and DC assemblages. Machine learning encompasses a variety of techniques that are ultimately rooted in pattern recognition (121). Included in this approach are powerful procedures for group identification and classification that can, when used with skeletal part profiles, discriminate among different agents of bone accumulation (122), a tactic we build on here.

NN (R libraries: "neuralnet" and "caret"). These algorithms, so named because of their comparability to the neural networks of mammalian brains, use regression methods to create interconnected nodes (i.e., a network) that are organized into layers. Patterns (group-specific abundances for all 23 skeletal elements, in this case) are presented to the network as an "input" layer and the weighted connections between nodes produce an "output" layer that reveals classifications. The network is trained through a resampling method that uses varying numbers of nodes (odd numbers between 1 and 19: 1, 3, 5, 7, etc.) on training and test subsamples, a process that adjusts the weights through successive layers of nodes to produce the most likely classification.

SVM (R libraries: "e1071" and "caret"). An SVM creates a mathematical and spatial boundary between data points in a multidimensional space. This boundary, referred to as a hyperplane, creates a homogenous distribution of data on either side. SVMs provide a powerful method of nonlinear classification because data separation is achieved with kernels, which add additional dimensions to data to achieve a sufficient separation according to class (groups of comparative assemblages, in this case). Here we utilize the C-SVM classification parameter with a radial kernel. The dimensions of the hyperplane are selected through the value of C. Large values produce a narrow plane that maximizes classification, while low values result in a wider plane and, thus, higher misclassification rates. We input a high value for C in the present analysis. As with the NN approach, the SVM learns through a training set and its accuracy is evaluated with a testing set.

Decision trees using the C5.0 algorithm (DTC50; R libraries: "C50" and "caret"). Decision trees operate through recursive partitioning of data, which means that model performance can be improved with metalearning methods. One such method is k-fold cross-validation. This involves the random division of the original dataset into training sets and testing sets k times. Because the results are averaged across trials, more divisions produce lower variance in classification estimates. The typical number of trials is 10, a standard we adopt here (i.e., a 10-fold cross-validation). The integration of the C5.0 algorithm into decision tree analysis enables accuracy rates comparable to the far more complex NN and SVM machine-learning methods. Importantly, DTC50 provides accurate results even when forced, as it is in this study, to work with small training sets.

K-nearest neighbor (KNN; R libraries: "class" and "knn"). This is an unsupervised learning algorithm that assigns unlabeled data to the class among k classes with the most similarly labeled examples. This algorithm performs well in situations with many variables and well-defined labeled sets. KNN also makes no assumptions about the sample distribution and is easily trained. While large k values tend to reduce variance bias, nuanced patterns may go unnoticed. We therefore opt for intermediate k values provided by the k-means analysis discussed above (three or four, in this case). The training sets and testing sets are created through boosted subsamples.

RF (R libraries: "randomForest" and "caret"). RF algorithms, unlike the other methods described above, use random subsets of variables (skeletal elements, in this case), each of which produces an independent tree. Bootstrap aggregation, more commonly known as bagging, is the most common RF procedure, which splits a training set into multiple datasets derived from bootstrapping.

The results are compared with a validation test derived from those observations (usually about one third; referred to as out-of-bag) not used for the training set. The RF then estimates how many iterations, or trees, are needed to minimize the out-of-bag error. The algorithm averages the results across the trees to produce a robust classification method that avoids data overfitting, which is a common problem with standard decision and regression trees. Here, forests are built with 500 trees.

Each of the machine learning models are built with all 23 skeletal elements from only the 14 comparative assemblages, which are then used to classify the SH and DC samples. Before model construction, all skeletal part data undergo center and scale transformation. Because the sample of comparative assemblages is small, it must be carefully analyzed for cost and, if necessary, boosted, before it can be split into training sets and testing sets. Therefore, each of the model parameters is tuned, which involves the selection of a range of values for each parameter and the creation of multiple models through resampling. We resample the data 30 times to yield 30 different models for each machine-learning method. To choose the best model for analysis, we use Monte-Carlo leave-group-out cross-validation resampling. This creates multiple training set/testing set splits and is more robust with small samples than bootstrapping, bagging, and k-fold cross-validation methods (121).

The models produced by each machine learning method after 30 iterations are evaluated with Cohen's  $\kappa$ . Cohen's  $\kappa$ , which ranges from 0 to 1, is a more robust measure of prediction and classification than accuracy because it represents the degree of similarity between datasets corrected by chance. Cohen's  $\kappa$  is also used to identify the most reliable classification of the SH and DC hominin assemblages. Finally, we perform an unsupervised CA with PCA loading scores.

Additional Evaluation of Formation Scenarios. The geological evidence from the SH and DC seems to eliminate the possibility that corpses were transported into the caves through abiotic agents. The sites' taxonomic representation—hominins and carnivores only in the case of the SH, hominins only in the case of the DC in fact suggests highly selective biotic agents of accumulation. What is more, the cavities would likely have been inaccessible to all but the most agile or scansorial animals, just as they are today (5, 10). Indeed, a fall into the SH was probably a one-way venture (5). Carnivore accumulation. Bears and lions are seen as the two most likely candidates for the modifications on and accumulation of the SH bones (6, 123). Typically, these carnivores are not highly selective predators nor do they transport and accumulate large bone collections. We thus agree with Sala et al. (123) and others (see, for example, ref. 4) that it is unlikely that the SH assemblage represents a primarily carnivore accumulation. If this is the case, the carnivore damage, and thus the creation of a biased skeletal part profile, must have occurred after the deposition of the hominin corpses within the SH cavity (123). We note, however, that a focus on human prey, and even the transport of human corpses over substantial distances, is not unheard of among modern lions (124). Such behavior may arise because of prey scarcity, traumatic injury that prevents the pursuit of other prey or, perhaps, the development of hunting traditions within local lion populations (125). Regardless, carnivore impact on the SH assemblage is probably more intense than that proposed by Sala et al. (123). Barring the discovery of an alternative entrance into the DC, the narrow access points of the current passage make it extremely unlikely that the hominins were transported in by a large carnivore. The absence of carnivore damage, keeping in mind the poor cortical preservation of the DC bones, also does not support the carnivore accumulation hypothesis.

*Natural accumulation/death trap.* Skeletal part and demographic data strongly suggest that the SH operated as a natural death trap over many years for the numerous bear and fox individuals recovered

from the site (126). Drawn possibly by the promise of shelter or a scavengable morsel, carnivores in fact still become entrapped within the chamber today (4). Although the geological evidence indicates that the hominin corpses accumulated in a single depositional event, the demographic profile, dominated as it is by adolescents and young adults, is not consistent with mass catastrophic mortality (1). The DC hominins, on the other hand, probably accumulated over an extended period of time in multiple depositional episodes and are represented by all age classes, from infant to old adult (10). Perhaps the strongest evidence for a natural accumulation is the clustering of both the SH and DC skeletal part frequencies with the Misgrot Cave baboons. Dirks et al. (10, 11) seriously consider the possibility of repeated mortality events involving small groups of hominins, a description that closely mirrors the situation at Misgrot Cave. The biased baboon element frequencies may be due to sporadic carnivore involvement as evidenced by low rates of toothmarking (<2%, or about 20 of 1,000 specimens from the assemblage). We note, too, that baboon skeletal material is preserved in breccias within a side passage of the cave, which indicates accumulation over a relatively long interval (C14 dates on bones from the cave, which range from ~400 to ~30 y ago,

- Bermúdez de Castro JM, Martinón-Torres M, Lozano M, Sarmie S (2004) Paleodemography of the Atapuerca-Sima de los Huesos hominin sample: A revision and new approaches to the paleodemography of the European Middle Pleistocene population. J Anthropol Res 60:5–26.
- Arnold LJ, et al. (2014) Luminescence dating and palaeomagnetic age constraint on hominins from Sima de los Huesos, Atapuerca, Spain. J Hum Evol 67:85–107.
- Cuenca-Bescós G, et al. (2016) Updated Atapuerca biostratigraphy: Small-mammal distribution and its implications for the biochronology of the Quaternary in Spain. C R Palevol 15:621–634.
- Arsuaga JL, et al. (1997) Sima de los Huesos (Sierra de Atapuerca, Spain). The site. J Hum Evol 33:109–127.
- Aranburu A, Arsuaga JL, Sala N (2017) The stratigraphy of the Sima de los Huesos (Atapuerca, Spain) and implications for the origin of the fossil hominin accumulation. Quat Int 433:5–21.
- Andrews P, Fernández Jalvo Y (1997) Surface modifications of the Sima de los Huesos fossil humans. J Hum Evol 33:191–217.
- Carbonell E, Mosquera M (2006) The emergence of a symbolic behaviour: The sepulchral pit of Sima de los Huesos, Sierra de Atapuerca, Burgos, Spain. C R Palevol 5:155–160.
- 8. Dirks PHGM, et al. (2017) The age of *Homo naledi* and associated sediments in the Rising Star Cave, South Africa. *eLife* 6:e24231.
- 9. Berger LR, et al. (2015) Homo naledi, a new species of the genus Homo from the Dinaledi Chamber, South Africa. eLife 4:e09560.
- Dirks PHGM, et al. (2015) Geological and taphonomic context for the new hominin species Homo naledi from the Dinaledi Chamber, South Africa. eLife 4:e09561.
- Dirks PHGM, et al. (2016) Comment on "Deliberate body disposal by hominins in the Dinaledi Chamber, Cradle of Humankind, South Africa?" [J. Hum. Evol. 96 (2016) 145-148]. J Hum Evol 96:149–153.
- 12. Randolph-Quinney PS, et al. (2016) Response to Thackeray (2016)—The possibility of lichen growth on bones of *Homo naledi*: Were they exposed to light? *S Afr J Sci* 112:
- Hawks J, et al. (2017) New fossil remains of Homo naledi from the Lesedi Chamber, South Africa. eLife 6:e24232.
- Boot AM, de Ridder MAJ, Pols HAP, Krenning EP, de Muinck Keizer-Schrama SMPF (1997) Bone mineral density in children and adolescents: Relation to puberty, calcium intake, and physical activity. J Clin Endocrinol Metab 82:57–62.
- Littleton J, et al. (2012) Taphonomic analysis of Bronze Age burials in Mongolian khirigsuurs. J Archaeol Sci 39:3361–3370.
- Bello SM, Andrews P (2006) The intrinsic pattern of preservation of human skeletons and influence on the interpretation of funerary behaviours. The Social Archaeology of Funerary Remains. eds Gowland R. Knüsel C (Oxbow Books. Oxford). pp 1–13.
- Haglund WD (1991) Applications of taphonomic models to forensic investigations. PhD dissertation (University of Washington, Seattle, WA).
- Pickering TR, Carlson KJ (2004) Baboon taphonomy and its relevance to the investigation of large felid involvement in human forensic cases. Forensic Sci Int 144:37–44.
- Pickering TR, Heaton JL, Zwodeski SE, Kuman K (2011) Taphonomy of bones from baboons killed and eaten by wild leopards in Mapungubwe National Park, South Africa. J Taphon 9:117–159.
- 20. Martini JEJ, Keyser A (1989) Misgrot. Bull South African Speleol Assoc 30:47–48.
- 21. Trinkaus E (1985) Cannibalism and burial at Krapina. J Hum Evol 14:203–216.
- Schaafsma CF (2007) Appendix D. Compilation of excavated and previously reported ceramics from Pottery Mound. New Perspectives on Pottery Mound Pueblo, ed Schaasfsma P (Univ of New Mexico Press, Albuquerque, NM).
- Schaafsma P (2007) The Pottery Mound murals and rock art: Implications for regional interaction. New Perspectives on Pottery Mound Pueblo, ed Schaafsma P (Univ of New Mexico Press, Albuquerque, NM), pp 137–166.

also support this assertion). Of course, this comparison should not downplay what are significant geomorphological differences between Misgrot Cave and the SH and DC. Although entry to Misgrot Cave involves a challenging vertical climb, it is directly accessible to the surface whereas the hominin locales require significantly more difficult or circuitous treks. This is particularly true of the DC, which is located well within the dark zone of the Rising Star Cave System. Nevertheless, we think natural accumulation coupled with a low level of postdepositional carnivore involvement should continue to be a viable formation model for the SH (see also ref. 127) and, especially, the DC.

Anthropogenic accumulation. A combination of restrictive taxonomic representation, high hominin MNIs, and geological and taphonomic considerations makes deliberate disposal a reasonable hypothesis for the deposition of the SH and DC hominins. The skeletal element data, though, suggest that the corpses experienced some disturbance before and/or after their initial deposition within the cave chambers. Carnivore consumption can readily explain the biased abundances for the SH and remains a definite possibility for the DC, although other processes such as diagenetic attrition, trampling, sampling bias, and the removal of material through floor drains, should not be discounted.

- Schorsch RLG (1962) The physical anthropology of Pottery Mound: A Pueblo IV site in west central New Mexico. Master's thesis (University of New Mexico, Albuquerque, NM)
- Akins NJ, Hannaford CA (2005) Archaeological Testing at Kuaua Pueblo, Coronado State Monument, New Mexico (Museum of New Mexico, Office of Archaeological Studies. Sante Fe. NM).
- 26. Luhrs DL, Ely AG (1939) Burial customs at Kuaua. Palacio 46:27-32.
- Karhu SL (2003) Appendix B1: Osteological analysis of human remains. From Dancing Man to Hummingbird: Long-Term Prehistoric Change in Southwest Colorado. Volume 3, Appendix B1 and B2: Pueblo I - Pueblo III Sites, ed Chenault ML (SWCA Environmental Consultants, Broomfield, CO), pp 1–57.
- Trinkaus E (2006) The upper limb remains. Early Modern Human Evolution in Central Europe: The People of Dolní Věstonice and Pavlov, eds Trinkaus E, Svoboda J (Oxford Univ Press, Oxford), pp 327–372.
- Trinkaus E (2006) The lower limb remains. Early Modern Human Evolution in Central Europe: The People of Dolní Věstonice and Pavlov, eds Trinkaus E, Svoboda J (Oxford Univ Press, Oxford), pp 380–418.
- Holliday TW, Hillson SW, Franciscus RG, Trinkaus E (2006) The human remains: A summary inventory. Early Modern Human Evolution in Central Europe: The People of Dolní Věstonice and Pavlov, eds Trinkaus E, Svoboda J (Oxford Univ Press, Oxford), pp 27–30.
- Holliday TW (2006) The costal skeletons. Early Modern Human Evolution in Central Europe: The People of Dolní Věstonice and Pavlov, eds Trinkaus E, Svoboda J (Oxford Univ Press. Oxford), pp 295–326.
- 32. Hillson SW, Franciscus RG, Holliday TW, Trinkaus E (2006) The ages at death. Early Modern Human Evolution in Central Europe: The People of Dolní Věstonice and Pavlov. eds Trinkaus E. Svoboda J (Oxford Univ Press. Oxford). pp 31–45.
- 33. McCown TD, Keith A (1939) The Stone Age of Mount Carmel. Volume II: The Fossil Human Remains from the Levalloiso-Mousterian (Clarendon, Oxford).
- Grün R, et al. (2005) U-series and ESR analyses of bones and teeth relating to the human burials from Skhul. J Hum Evol 49:316–334.
- McCown TD (1937) Mugharet es-Skhül: Description and excavation. The Stone Age of Mount Carmel, eds Garrod DA, Bate D (Clarendon, Oxford), pp 91–107.
- 36. Pettitt PB (2011) *The Palaeolithic Origins of Human Burial* (Routledge, Abington, PA).
- Smirnov Y (1989) Intentional human burial: Middle Paleolithic (last glaciation) beginnings. J World Prehist 3:199–233.
- ginnings. J World Prenist 3:199–233.

  38. Vandermeersch B (1981) Les Hommes Fossiles de Qafzeh (Israël) (Éditions du Centre
- National de la Recherche Scientifique, Paris).
  39. Madelaine S, et al. (2008) Nouveaux restes humains moustériens rapportés au squelette néandertalien de Regourdou 1 (Regourdou, commune de Montignac, Dordogne, France). Paleo 20:101–114.
- Gómez-Olivencia A, Couture-Veschambre C, Madelaine S, Maureille B (2013) The vertebral column of the Regourdou 1 Neandertal. J Hum Evol 64:582–607.
- Gómez-Olivencia A (2013) Back to the old man's back: Reassessment of the anatomical determination of the vertebrae of the Neandertal individual of La Chapelleaux-Saints. Ann Paleontol 99:43–65.
- Rendu W, et al. (2014) Evidence supporting an intentional Neandertal burial at La Chapelle-aux-Saints. Proc Natl Acad Sci USA 111:81–86.
- 43. Trinkaus E (1983) The Shanidar Neandertals (Academic, New York).
- 44. Reynolds T, et al. (2016) New investigations at Shanidar Cave, Iraqi Kurdistan. The Archaeology of the Kurdistan Region of Iraq and Adjacent Region eds Kopanias K, MacGinnis J (Archaeopress, Oxford), pp 369–372.
- Tillier A-M (1991) La mandubile et les dents. Le Squelette Moustérian de Kebara 2, eds Bar-Yosef O, Vandermeersch B (Éditions du Centre National de la Recherche Scientifíque, Paris), pp 97–111.

- Arensburg B (1991) The vertebral column, thoracic cage and hyoid bone. Le Squelette Moustérian de Kebara 2, eds Bar-Yosef O, Vandermeersch B (Éditions du Centre National de la Recherche Scientifíque, Paris), pp 113–146.
- Rak Y (1991) The pelvis. Le Squelette Moustérian de Kebara 2, eds Bar-Yosef O, Vandermeersch B (Éditions du Centre National de la Recherche Scientifíque, Paris), pp 147–156.
- Vandermeersch B (1991) La ceinture scapulaire et les membres supérieurs. Le Squelette Moustérian de Kebara 2, eds Bar-Yosef O, Vandermeersch B (Éditions du Centre National de la Recherche Scientifíque, Paris), pp 157–178.
- Carretero JM, et al. (2015) The Magdalenian human remains from El Mirón Cave, Cantabria (Spain). J Archaeol Sci 60:10–27.
- Smith FH The Neandertal Remains from Krapina: A Descriptive and Comparative Study (Department of Anthropology, Univ of Tennessee, Knoxville, TN).
- Trinkaus E (1975) The Neandertals from Krapina, northern Yugoslavia: An inventory
  of the lower limb remains. Z Morphol Anthropol 67:44–59.
- Rink WJ, Schwarcz HP, Smith FH, Radovĉić J (1995) ESR ages for Krapina hominids. Nature 378:24.
- Ullrich H (2006) Krapina-A mortuary practice site with cannibalistic rites. Period Biol 108:501–517.
- Gorjanović-Kramberger K (1901) Der paläolithische Mensch und seine Zeitgnossen aus dem Diluvium von Krapina in Kroatien. Mitteilung der Anthropol Gesellschaft Wien 31:164–197.
- 55. Gorjanović-Kramberger K (1906) Der Diluviale Mensch von Krapina in Kroatien (CW Kreidel, Wiesbaden, Germany).
- Russell MD (1987) Mortuary practices at the Krapina Neandertal site. Am J Phys Anthropol 72:381–397.
- 57. Russell MD (1987) Bone breakage in the Krapina hominid collection. *Am J Phys Anthropol* 72:373–379.
- 58. Villa P, et al. (1986) Un cas de cannibalisme au Néolithique. *Gall Préhistoire* 29: 143-171
- Le Bras-Goude G, Binder D, Zemour A, Richards MP (2010) New radiocarbon dates and isotope analysis of Neolithic human and animal bone from the Fontbrégoua Cave (Salernes, Var, France). J Anthropol Sci 88:167–178.
- 60. Bahn PG (1990) Eating people is wrong. Nature 348:395.
- 61. Villa P, Courtin J (1991) Cannibalism in the Neolithic. Nature 351:613-614.
- Bermúdez de Castro JM, et al. (2017) Homo antecessor: The state of the art eighteen years later. Quat Int 433:22–31.
- 63. Bermúdez de Castro JM, et al. (2012) Early Pleistocene human humeri from the Gran Dolina-TD6 site (Sierra de Atapuerca, Spain). Am J Phys Anthropol 147:604–617.
  64. Carretero JM, Lorenzo C, Arsuaga JL (1999) Axial and appendicular skeleton of
- Carretero JM, Lorenzo C, Arsuaga JL (1999) Axial and appendicular skeleton of Homo antecessor. J Hum Evol 37:459–499.
- 65. Gómez-Olivencia A, et al. (2010) The costal skeleton of *Homo antecessor*: Preliminary results. *J Hum Evol* 59:620–640.
- Lorenzo C, Arsuaga JL, Carretero JM (1999) Hand and foot remains from the Gran Dolina Early Pleistocene site (Sierra de Atapuerca, Spain). J Hum Evol 37:501–522.
- Pablos A, et al. (2012) New foot remains from the Gran Dolina-TD6 Early Pleistocene site (Sierra de Atapuerca, Burgos, Spain). J Hum Evol 63:610–623.
- Moreno D, et al. (2015) New radiometric dates on the lowest stratigraphical section (TD1 to TD6) of Gran Dolina site (Atapuerca, Spain). Quat Geochronol 30: 535–540.
- Fernández-Jalvo Y, Carlos Díez J, Cáceres I, Rosell J (1999) Human cannibalism in the Early Pleistocene of Europe (Gran Dolina, Sierra de Atapuerca, Burgos, Spain). J Hum Evol 37:591–622.
- Saladié P, et al. (2011) Carcass transport decisions in Homo antecessor subsistence strategies. J Hum Evol 61:425–446.
- Carbonell E, et al. (2010) Cultural cannibalism as a paleoeconomic system in the European Lower Pleistocene: The case of level TD6 of Gran Dolina (Sierra de Atapuerca, Burgos, Spain). Curr Anthropol 51:539–549.
- Saladié P, et al. (2014) The role of carnivores and their relationship to hominin settlements in the TD6-2 level from Gran Dolina (Sierra de Atapuerca, Spain). Quat Sci Rev 93:47–66.
- Cáceres I, Lozano M, Saladié P (2007) Evidence for bronze age cannibalism in El Mirador Cave (Sierra de Atapuerca, Burgos, Spain). Am J Phys Anthropol 133:899–917.
- Bello SM, Saladié P, Cáceres I, Rodríguez-Hidalgo A, Parfitt SA (2015) Upper Palaeolithic ritualistic cannibalism at Gough's Cave (Somerset, UK): The human remains from head to toe. J Hum Evol 82:170–189.
- 75. Hawkey DE (2003) Human dental remains from Gough's Cave (Somerset, England). Bull Nat Hist Museum 58(Suppl):23–35.
- Churchill SE (2001) The Crewsellian (Pleistocene) human upper limb remains from Gough's Cave (Somerset, England). Bull Nat Hist Museum 57:7–24.
- Malville NJ (1989) Two fragmented human bone assemblages from Yellow Jacket, southwestern Colorado. Kiva 55:3–22.
- 78. Billman BR, Lambert PM, Leonard BL (2000) Cannibalism, warfare, and drought in the Mesa Verde Region during the twelfth century A.D. *Am Antiq* 65:145–178.
- Lambert PM, Billman BR, Leonard BL (2000) Explaining variability in mutilated human bone assemblages from the American Southwest: A case study from the southern piedmont of Sleeping Ute Mountain, Colorado. Int J Osteoarchaeol 10:49–64.
- 80. Ubelaker DH (1997) Skeletal Biology of Human Remains from La Tolita, Esmeraldas Province, Ecuador (Smithsonian Instution Press, Washington, DC).
- 81. Willey PS (1990) Prehistoric Warfare on the Great Plains: Skeletal Analysis of the Crow Creek Massacre Victims (Garland Publishing, New York).
- Kimbel WH, Johanson DC, Coppens Y (1982) Pliocene hominid cranial remains from the Hadar Formation, Ethiopia. Am J Phys Anthropol 57:453–499.
- 83. White TD, Johanson DC (1982) Pliocene hominid mandibles from the Hadar Formation, Ethiopia: 1974–1977 collections. *Am J Phys Anthropol* 57:501–544.

- Lovejoy CO, Johanson DC, Coppens Y (1982) Hominid upper limb bones recovered from the Hadar Formation: 1974–1977 collections. Am J Phys Anthropol 57:637–649.
- Lovejoy CO, Johanson DC, Coppens Y (1982) Elements of the axial skeleton recovered from the Hadar Formation: 1974–1977 collections. Am J Phys Anthropol 57:631–635.
- Lovejoy CO, Johanson DC, Coppens Y (1982) Hominid lower limb bones recovered from the Hadar formation: 1974–1977 collections. Am J Phys Anthropol 57: 679–700
- 87. Ward CV, Kimbel WH, Harmon EH, Johanson DC (2012) New postcranial fossils of Australopithecus afarensis from Hadar, Ethiopia (1990–2007). J Hum Evol 63:1–51.
- Ward CV, Kimbel WH, Johanson DC (2011) Complete fourth metatarsal and arches in the foot of Australopithecus afarensis. Science 331:750–753.
- Bush ME, Lovejoy CO, Johanson DC, Coppens Y (1982) Hominid carpal, metacarpal, and phalangeal bones recovered from the Hadar Formation: 1974–1977 collections. Am J Phys Anthropol 57:651–677.
- Latimer BM, Lovejoy CO, Johanson DC, Coppens Y (1982) Hominid tarsal, metatarsal, and phalangeal bones recovered from the Hadar Formation: 1974–1977 collections. Am J Phys Anthropol 57:701–719.
- Walter RC (1994) Age of Lucy and the first family: Single-crystal 40Ar/39Ar dating of the Denen Dora and lower Kada Hadar members of the Hadar Formation, Ethiopia. Geology 22:6–10.
- Johanson DC, Taieb M, Coppens Y (1982) Pliocene hominids from the Hadar Formation, Ethiopia (1973–1977): Stratigraphic, chronologic, and paleoenvironmental contexts, with notes on hominid morphology and systematics. Am J Phys Anthropol 57:373–402.
- Behrensmeyer AK (2008) Paleoenvironmental context of the Pliocene A.L. 333 "First Family" hominin locality, Hadar Formation, Ethiopia. The Geology of Early Humans in the Horn of Africa, eds Quade J, Wynn JG (Geological Society of America, Boulder, CO), pp 203–214.
- Radosevich SC, Retallack GJ, Taieb M (1992) Reassessment of the paleoenvironment and preservation of hominid fossils from Hadar, Ethiopia. Am J Phys Anthropol 87:15–27.
- White TD, Johanson DC (1989) The hominid composition of Afar Locality 333: Some preliminary observations. Hominidae: Proceedings of the Second International Congress of Human Paleontology, ed Giacobini G (Jaca Book, Milan), pp 97–101.
- Brown P, et al. (2004) A new small-bodied hominin from the Late Pleistocene of Flores, Indonesia. Nature 431:1055–1061.
- Morwood MJ, Jungers WL (2009) Conclusions: Implications of the Liang Bua excavations for hominin evolution and biogeography. J Hum Evol 57:640–648.
- Larson SG, et al. (2009) Descriptions of the upper limb skeleton of Homo floresiensis.
   J Hum Evol 57:555–570.
- Jungers WL, et al. (2009) Descriptions of the lower limb skeleton of Homo floresiensis. J Hum Evol 57:538–554.
- Morwood MJ, et al. (2005) Further evidence for small-bodied hominins from the Late Pleistocene of Flores, Indonesia. Nature 437:1012–1017.
- Jungers WL (2013) Homo floresiensis. A Companion to Paleoanthropology, ed Begun DR (Wiley-Blackwell, Oxford), pp 582–598.
- Orr CM, et al. (2013) New wrist bones of Homo floresiensis from Liang Bua (Flores, Indonesia). J Hum Evol 64:109–129.
- Lordkipanidze D, et al. (2013) A complete skull from Dmanisi, Georgia, and the evolutionary biology of early Homo. Science 342:326–331.
- Lordkipanidze D, et al. (2007) Postcranial evidence from early Homo from Dmanisi, Georgia. Nature 449:305–310.
- Lordkipanidze D, et al. (2005) Anthropology: The earliest toothless hominin skull. Nature 434:717–718.
- Gabunia L, et al. (2000) Earliest Pleistocene hominid cranial remains from Dmanisi, Republic of Georgia: Taxonomy, geological setting, and age. Science 288:1019–1025.
- 107. Berger LR, et al. (2010) Australopithecus sediba: A new species of Homo-like australopith from South Africa. Science 328:195–204.
  108. de Ruiter DJ, et al. (2013) Mandibular remains support taxonomic validity of Australopith
- tralopithecus sediba. Science 340:1232997.

  109. Churchill SE, et al. (2013) The upper limb of Australopithecus sediba. Science 340:
- Churchill SE, et al. (2013) The upper limb of Australopithecus sediba. Science 340: 1233477.
- Kivell TL, Kibii JM, Churchill SE, Schmid P, Berger LR (2011) Australopithecus sediba hand demonstrates mosaic evolution of locomotor and manipulative abilities. Science 333:1411–1417.
- 111. Zipfel B, et al. (2011) The foot and ankle of Australopithecus sediba. Science 333: 1417-1420.
- Carson EA, Stefan VH, Powell JF (2000) Skeletal manifestations of bear scavenging. J Forensic Sci 45:515–526.
- Pickering TR (2001) Carnivore voiding: A taphonomic process with the potential for the deposition of forensic evidence. J Forensic Sci 46:406–411.
- 114. Arsuaga JL, et al. (2015) Postcranial morphology of the middle Pleistocene humans from Sima de los Huesos, Spain. *Proc Natl Acad Sci USA* 112:11524–11529.
- 115. Pablos A, Pantoja-Pérez A, Martínez I, Lorenzo C, Arsuaga JL (2017) Metric and morphological analysis of the foot in the Middle Pleistocene sample of Sima de los Huesos (Sierra de Atapuerca, Burgos, Spain). Quat Int 433:103–113.
- Pablos A, et al. (2013) Human talus bones from the Middle Pleistocene site of Sima de los Huesos (Sierra de Atapuerca, Burgos, Spain). J Hum Evol 65:79–92.
- Pablos A, et al. (2014) Human calcanei from the Middle Pleistocene site of Sima de los Huesos (Sierra de Atapuerca, Burgos, Spain). J Hum Evol 76:63–76.
- 118. Feuerriegel EM, et al. (2017) The upper limb of Homo naledi. J Hum Evol 104: 155–173.
- 119. Lantz B (2013)  $\it Machine\ Learning\ with\ R$  (Packt Publishing, Birmingham, UK).
- 120. Hair JF, Tatham RL, Anderson RE, Black W (1998) Multivariate Data Analysis (Prentice Hall, Upper Saddle River, NJ).

- Arriaza MC, Domínguez-Rodrigo M (2016) When felids and hominins ruled at Olduvai Gorge: A machine learning analysis of the skeletal profiles of the nonanthropogenic Bed I sites. Quat Sci Rev 139:43–52.
- 123. Sala N, Arsuaga JL, Martínez I, Gracia-Téllez A (2014) Carnivore activity in the Sima de los Huesos (Atapuerca, Spain) hominin sample. *Quat Sci Rev* 97:71–83.
- 124. Rushby G (1965) No More the Tusker (W. H. Allen, London).

- 125. Kerbis Peterhans JC, Gnoske TP (2001) The science of "man-eating" among lions Panthera leo with a reconstruction of the natural history of the "man-eaters of Tsavo.". J East Afr Nat Hist 90:1–40.
- 126. García N, Arsuaga JL, Torres T (1997) The carnivore remains from the Sima de los Huesos Middle Pleistocene site (Sierra de Atapuerca, Spain). J Hum Evol 33:155–174.
- 127. Rabadá D (2015) Taphonomical interpretation of the Sima de los Huesos site (Atapuerca range, Burgos, Spain): A review. Spanish J Palaeontol 30:79–94.

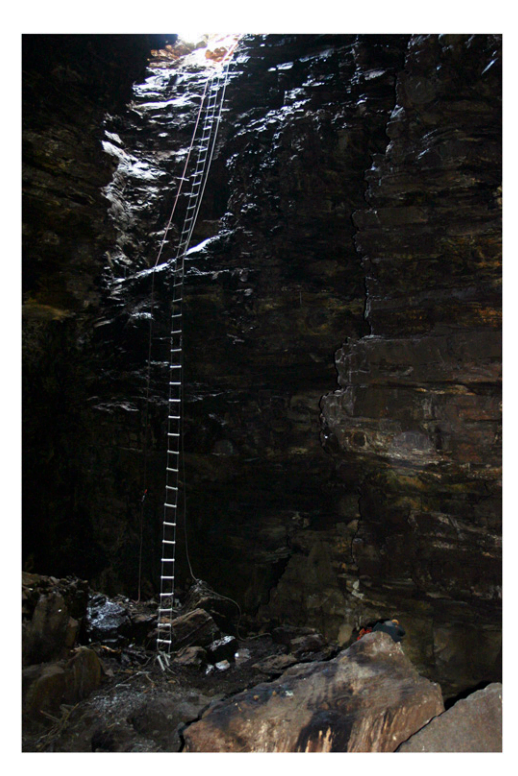


Fig. S1. Vertical entrance into Misgrot. Standing within the cave, one can observe the near 17-m vertical drop along the cave's northern extent (with light from outside appearing near the top). Abseiling equipment was required to move into and out of the cave. Photo courtesy of J.L.H.



Fig. S2. Mummified male baboon. This nearly complete male baboon was recovered ~4 m from the northern entrance shown in Fig. S1. Note the accumulation of baboon dung around the skeletal remains as well as brush (lying on top of the skeleton). The edge of the western wall can be seen in the background. A 10-cm scale is shown along the bottom of the figure with an arrow and number written on it. The number was used to identify the specimen (#1, shown here) while the arrow indicates the direction of magnetic north. The baboon's head (seen on the extreme right of the picture) is upslope (on the talus). Photo courtesy of J.L.H.



Fig. S3. Disarticulated baboon remains. Among the baboon dung and marula seeds, an isolated right radius (*Left*) and a mummified, complete left upper limb, including scapula (*Right*) can be seen. These remains were found farther (an additional 6 m) down the talus slope from the mummified baboon (#1, near the entrance). As elements progressed down the talus slope, the remains became more disarticulated, so that by the time they reached the farthest extent, they were single isolated elements (e.g., a single cervical vertebra). Photo courtesy of J.L.H.

Table S1. Skeletal element abundance data (tallied by %MAU) for the fossil and modern assemblages

											%МАП										
Assemblage	CRN	MR	Ħ	Ŧ	ΓM	SAC	ST	RB C	CLA S	SC HM	√ RD	IN .	Ð	모	Σ	FM	PT	ΔT	FB	T	E
Fossil assemblage/component Primary interment																					
Pottery Mound: Pueblo IV	88.4	79.1	84.4	87.6	89.8	2.06	0.0	87.3 9.	94.2 90	90.7 84.	68	.5 86.0	75.6	75.1	89.5	100.0	79.1	76.7	79.1	72.1	49.8
Kuaua Pueblo: Pueblo IV	100.0	94.1	60.5	65.4	74.1	76.5	0.0	60.8	75.7 77	77.2 94.	9.68 6.	.0 80.1	35.7	46.2	88.2	97.8	55.6	89.0	76.5	60.1	33.7
Component (MNI = 84)																					
Possible primary interment																					
Mugharet es-Skhūl: Layer B (MNI = 7)	100.0 100.0	100.0	20.0	40.0	48.0	7 0.09	40.0	27.5 6	60.0 40	40.0 90.0	0.08 0.	0.06 0.	27.5	18.4	70.0	80.0	20.0	90.0	70.0	31.4	15.3
Cannibalism/secondary interment																					
Fontbrégoua: Feature H1 (MNI = 7)	100.0	85.7	8.2	0.0	0.0	0.0		0.0			.4 14.3		0.0		0.0	21.4	0.0	14.3	21.4	2.0	8.0
Fontbrégoua: Feature H3 (MNI = 6)	0.0	0.0	6.3	0.0	0.0	22.				299 299					11.1	44.4	0.0	100.0	33.3	0.0	0.0
Gran Dolina: TD6 Level (MNI $= 2$ )	0.0	100.0	14.3	0.0	0.0	0.0	0.0						6.3	9.5	0.0	25.0	50.0	0.0	0.0	7.1	13.2
El Mirador Cave: MIR4A (MNI = 5)	100.0	80.0	2.9	10.0	8.0	0.0			0.0	10.0 10.0	0.0	.0 20.0			0.0	10.0	0.0	20.0	20.0	4.3	0.0
Krapina (MNI = $20$ )	100.0	0.09	15.7	5.0	21.0	0.0	0.0	3.1 2					0.3	8.9	30.0	35.0	37.5	32.5	35.0	6.4	5.8
Nonanthropogenic																					
A.L. 333: Denen Dora	66.7	100.0	9.5	2.8	3.3	0.0	0.0	2.8	16.7 0	0.0 33.3		8.3 33.3	4.2	19.3	0.0	41.7	0.0	33.3	33.3	10.7	13.2
Member (MNI = $17$ )																					
Possible disposal																					
Sima de los Huesos (MNI = $18$ )	86.7	100.0	40.0	25.6	25.3	33.3	26.7 1	16.7 3		46.7 40.0		7 43.3	39.2	43.2	0.09	30.0	36.7	33.3	30.0	49.5	32.6
Dinaledi Chamber (MNI = 15)	85.7	100.0	14.3	15.5	9.8	14.3	14.3 1		35.7 35	35.7 57.1				35.0	64.3	100.0	28.6	64.3	57.1	34.7	24.8
Modern assemblages																					
Human corpses																					
Unscavenged (MNI = $17$ )	84.2	89.5	89.5	89.0	84.2		73.7 8				.2 100.0	0 81.6		64.7	89.5	89.5	76.3	86.8	86.8	43.2	56.2
Scavenged (MNI = $45$ )	100.0	88.6	73.7	79.2	81.8	77.3 (	61.4 7	71.3 6	61.4 62	62.5 54.	.5 50.0	.0 44.3	26.7	26.7	78.4	73.9	38.6	64.8	58.0	27.8	35.6
Leopard refuse																					
Leopard feeding (observed) (MNI $= 8$ )	100.0	100.0	23.2	20.0	25.4	20.0	0.0	28.6		50.0 93.8	.8 68.8	8.89	18.8	26.0	62.5	93.8	0.0	93.8	8.89	31.3	26.0
Mapungubwe leopard kills	100.0	85.7	26.5	38.1	85.7				14.3 50							92.9	21.4	78.6	64.3	26.5	20.7
(inferred) ( $MNI = 7$ )																					
Natural baboon accumulation	,		,													i	;	,	:		!
Misgrot Cave (MNI = $7$ )	100.0	57.1	38.8	27.4	22.3	78.6	14.3 2	24.4 2	21.4 71	71.4 71.4	.4 42.9	9 57.1	19.0	19.7	42.9	71.4	14.3	35.7	14.3	14.3	19.7

Skeletal element abbreviations: CE, cervical; CLA = clavicle; CP, carpals; CRN, cranium; FB, fibula; FT, foot (including metatarsals and pedal phalanges) FM, femur; HD, hand (includes metacarpals and manual phalanges); HM, humerus; IM, innominate; LM, lumbar; MAU, minimum animal units; MR, mandible; PT, patella; RB, rib; RD, radius; SAC, sacrum; SC, scapula; ST, sternum; TA, tibia; TH, thoracic; TR, tarsals; UL, ulna.

## **Other Supporting Information Files**

Dataset S1 (XLSX)